

The relaxor enigma – charge disorder and random fields in ferroelectrics

WOLFGANG KLEEMANN

Angewandte Physik, Universität Duisburg-Essen, D-47048 Duisburg, Germany

Substitutional charge disorder giving rise to quenched electric random-fields (*RF*s) is probably at the origin of the peculiar behavior of *relaxor* ferroelectrics, which are primarily characterized by their strong frequency dispersion of the dielectric response and by an apparent lack of macroscopic symmetry breaking at the phase transition. Spatial fluctuations of the *RF*s correlate the dipolar fluctuations and give rise to polar nanoregions in the paraelectric regime as has been evidenced by piezoresponse force microscopy (PFM) at the nanoscale. The dimension of the order parameter decides upon whether the ferroelectric phase transition is destroyed (e.g. in cubic $\text{PbMg}_{1/3}\text{Nb}_{2/3}\text{O}_3$, PMN) or modified towards *RF* Ising model behavior (e.g. in tetragonal $\text{Sr}_{1-x}\text{Ba}_x\text{Nb}_2\text{O}_6$, SBN, $x \approx 0.4$). Frustrated interaction between the polar nanoregions in cubic *relaxors* gives rise to cluster glass states as evidenced by strong pressure dependence, typical dipolar slowing-down and theoretically treated within a spherical random bond-*RF* model. On the other hand, freezing into a domain state takes place in uniaxial *relaxors*. While at T_c non-classical critical behavior with critical exponents $\gamma \approx 1.8$, $\beta \approx 0.1$ and $\alpha \approx 0$ is encountered in accordance with the *RF* Ising model, below $T_c \approx 350$ K *RF* pinning of the walls of frozen-in nanodomains gives rise to non-Debye dielectric response. It is relaxation- and creep-like at radio and very low frequencies, respectively.

© 2006 Springer Science + Business Media, Inc.

1. Introduction

Relaxor ferroelectrics include a large group of solid solutions, mostly oxides, with a perovskite or tungsten bronze structure. In contrast to ordinary ferroelectrics (FE) whose physical properties are quite adequately described by the Landau-Ginzburg-Devonshire theory [1], *relaxors* possess the following main features: (i) a significant frequency-dependence of the electric permittivity, (ii) absence of both spontaneous polarization and structural macroscopic symmetry breaking, (iii) FE-like response arising after field cooling to low temperature [2].

Very high response coefficients and an enhanced width of the high response regime around the “ordering” temperature T_m , (“Curie range”) make *relaxors* popular systems for applications as piezoelectric/electrostrictive *actuators* and *sensors* (e.g. scanning probe microscopy, ink jet printer, adaptive optics, micromotors, vibration sensors/attenuators, Hubble telescope correction, ...) and as *electro-* or *elasto-optic* and *photorefractive elements* (segmented displays, modulators, image storage, holographic data storage, ...).

When reflecting on the occurrence of *relaxor* behavior in perovskites, there appear to be two essential ingredients:

- i. existence of *lattice disorder*,
- ii. existence of *polar nanoregions* at temperatures much higher than T_m .

The first ingredient can be taken for granted, since *relaxor* behavior in these materials does not occur in the absence of disorder. The second ingredient is manifested in many experimental observations common to all perovskite *relaxors*, as will be discussed later.

The following physical picture has emerged for *relaxors* and seems to be widely accepted. Chemical substitution and lattice defects introduce extra charges or dipolar entities in mixed ABO_3 perovskites. At very high temperatures, thermal fluctuations are so large that there are no well-defined dipole moments. However, on cooling, the presence of these dipolar entities manifests itself as small polar nanoregions below the so-called Burns

temperature, T_d [3]. These regions grow as the correlation length, r_c , increases with decreasing T , and finally, two different situations may arise. If the regions become large enough (macrodomains) so as to percolate (or permeate) the whole sample, then the sample will undergo a static, cooperative FE phase transition at T_c . On the other hand, if the nanoregions grow with decreasing T , but do not become large enough or percolate the sample, then they will ultimately exhibit a dynamic slowing down of their fluctuations at $T \leq T_m$ leading to an isotropic *relaxor* state with random orientation of the polar domains.

A matter of dispute is still the physical significance and the very origin of the Burns temperature. Very probably it is not a usual phase transitions temperature. It might rather be considered as a so-called Griffiths temperature, which signifies the onset of weak singularities in a diluted ferroic system below the transition temperature of the undiluted system [4, 5]. However, the sharp onset of weak singularities is not at all confirmed in *relaxor* systems. We rather believe that the temperature regime in which the domains grow in size is continuous and merely determined by the correlating forces due to the underlying quenched random field (*RF*) distribution [6] as will be discussed in the next chapter.

2. Polar nanoregions

While many researchers believe that the above mentioned ingredients for *relaxor* behavior to appear are more or less independent, we have argued [6] that the primary cause of *relaxor* behavior is the charge disorder, which is at the origin of the occurrence of polar nanoregions and their fluctuations within the highly polarizable lattice [7]. In order to describe disordered systems and to explore their basic thermodynamic behavior simple spin models are frequently used. The model Hamiltonian

$$H = - \sum_{\langle ij \rangle} J_{ij} S_i S_j - \sum_i h_i S_i \quad (1)$$

accounts for random interactions (or random bonds, *RBs*), J_{ij} , between nearest neighbor spins S_i and S_j , and for quenched random fields (*RFs*), h_i acting on the spins S_i . While the *RBs* are at the origin of spin glass behavior [8], *RFs* may give rise to disordered domain states provided that the order parameter has continuous symmetry [9]. This is easily shown with the help of energy arguments considering both the bulk energy decrease by fluctuations of the *RFs* and the energy increase due to the formation of domain walls. A remarkable exception, which does not necessarily lead to a disordered ground state, is the random-field Ising model (*RFIM*) system in $d = 3$ dimensions. Owing to its discontinuous spin symmetry, atomically thin domain walls are expected, which are energetically unfavorable. For this reason the *3d RFIM*

is expected to exhibit long-range order below the critical temperature T_c . However, as a tribute to the *RFs* new criticality due to a $T = 0$ fixed point [10] and strongly decelerated critical dynamics are encountered [11].

Unfortunately, the original idea [9] to realize a ferromagnetic *RFIM* by doping with random magnetic ions fails. Their spin dynamics always couples to that of the host system such that their dipolar fields cannot be regarded as quenched ones. Regrettably, there is no chance to dope a ferromagnet with *magnetic monopoles*, which might readily provide quenched local magnetic fields. Bearing this in mind, the situation should be much more favorable for the electric counterparts to ferromagnets, where electric charges may take the role of field-generating monopoles. Indeed, in FE systems electric charge disorder should easily give rise to quenched *RFs*. This was proposed previously in order to understand the peculiar *relaxor* behavior of the archetypical solid solution $\text{PbMg}_{1/3}\text{Nb}_{2/3}\text{O}_3$ (PMN) [12]. Unfortunately, apart from the expected extreme slowing-down of the *RFIM* [11], which is closely related to the *relaxor*-typical huge polydispersivity [2, 12], no *RFIM* criticality was observed. This is a consequence of the high pseudo-spin dimension of the polarization order parameter, \mathbf{P} . It has eight easy $\langle 111 \rangle$ directions in the cubic unit cell and thus quasi-continuous symmetry [6]. Clearly the search for an appropriate uniaxial FE (one-component order parameter $\pm P_z$, *i.e.* $n = 2$) with charge disorder seems advisable in order to materialize a proper ferroic *3d RFIM* system. Only recently [13] the uniaxial *relaxor* crystal $\text{Sr}_{0.61-x}\text{Ce}_x\text{Ba}_{0.39}\text{Nb}_2\text{O}_6$ (SBN61:Ce, $0 \leq x < 0.02$) has been found to fulfil the conditions of a ferroic *RFIM* (see Chap. 4).

Evidence for the existence of polar nanoregions well above T_m has come from high resolution TEM which also showed the growth of these regions with decreasing T [14]. The evidence is also prominently reflected in certain properties of these systems. To provide the context, recall that for relaxors in the absence of electrical bias there are random $+$ and $-$ fluctuations of the dipolar polarization so that $\sum P_d = 0$, *i.e.*, there is no measurable remanent polarization. However, $\sum P_d^2 \neq 0$, and we then expect the existence of these polar regions to be manifested in properties which depend on P^2 , *e.g.*, electrostriction which is reflected in the thermal expansion and the quadratic electro-optic effect, which is reflected in the refractive index, or birefringence. Indeed, both of these properties have provided quantitative measures of this polarization for the relaxors. The manifestation of the presence of polar nanodomains in strong relaxors in terms of the electro-optic effect was first demonstrated by Burns and Dacol [3] in measurements of the T dependence of the refractive index, n . For a normal ABO_3 FE crystal, starting in the high-temperature PE phase, n decreases linearly with decreasing T down to T_d at which point n deviates from

linearity. The deviation is proportional to the square of the polarization and increases as the polarization evolves with decreasing T . If the FE transition is of first order, then there is a discontinuity in n at T_c followed by the expected deviation. This qualitative picture is representative of the behavior of many perovskite FEs. However, in the case of relaxors, Burns and Dacol observed deviations from linear $n(T)$ well above T_m . These deviations can be quantitatively described by the relationship [3, 14]

$$\Delta n = \frac{(\Delta n_{11} + \Delta n_{12})}{3} = \left(\frac{n_0^3}{2}\right) \left[\frac{(g_{33} + 2g_{13})}{3}\right] P_d^2 \quad (2)$$

where the Δn 's are the changes in the parallel and perpendicular components of n , n_o is the index in the absence of polarization (P_d), and the g_{ij} are the quadratic electro-optic coefficients. The temperature at the onset of the deviation from linear $n(T)$, $T_d = 620$ K in the case of PMN, is the Burns temperature. Above this temperature, thermal fluctuations are so large that there are no well-defined dipolar regions or clusters. These regions nucleate at T_d by taking advantage of the statistical fluctuations of the RF s and grow on lowering T . Diffuse scattering and HRTEM results indicate that in PMN these regions grow from 2 to 3 nm in size above 400 K to ≈ 10 nm at ≈ 160 K ($T_m \approx 230$ K) [2]. Thus, they are much smaller than typical FE domains, which are orders of magnitude larger. The small size of these nanoregions explains why they cannot easily be detected by diffraction measurements and the bulk structures of PMN and most strong mixed ABO_3 relaxors remain cubic to both x -ray and neutron probes and to long wavelength photons down to lowest temperatures.

Evidence for the existence of polar nanoregions well above T_m in relaxors has also been deduced from the T dependence of the susceptibility. As noted earlier, it is well established that $\chi'(T)$ in the high temperature, cubic PE phase of ABO_3 FEs follows the Curie–Weiss law $\chi' = C/(T - \theta)$, where θ is the Curie–Weiss temperature, over a wide temperature range. However, $\chi'(T)$ of relaxors shows large deviations from this law for $T > T_m$. Deviation from Curie–Weiss response sets in upon nucleation of the polar nanoregions at T_d , and this deviation grows with decreasing T as the size of the regions and their correlations increase. It can be described by a modified Curie–Weiss law [15]

$$\chi = \frac{C[1 - q(T)]}{[T - \theta(1 - q(T))]}, \quad (3)$$

which relates $\chi(T)$ below T_f to the local “spin glass” order parameter q , which is a function of temperature [16, 17]. While $q \rightarrow 0$ above at $T > T_d$, it increases with decreasing temperature below T_d because of increased dipolar correlations [16]. In such a case the local order parameter due to correlations between neighboring polar domains of

polarization P_i and P_j is $q = \langle P_i P_j \rangle^{1/2}$. The “universal relaxor polarization” regime of relaxors, where an unusual T dependence of the susceptibility, $\chi' = C/(T - T_0)^2$, is observed [17], is essentially the regime where the Edwards–Anderson order parameter q reveals a marked temperature dependence.

3. Cubic relaxors

The archetypical perovskite-like lead-containing relaxor $Pb(Mg_{1/3}Nb_{2/3})O_3$ (PMN, ABO_3 space group $Pm\bar{3}m$) system has been known for fifty years [12]. As-grown PMN single crystals exhibit excellent crystalline properties with small mosaic spread ($\omega \leq 0.01^\circ$). However, on the nanometer scale there is a significant degree of chemical and structural disorder [18]. Fig. 1 shows a random distribution of B site ions on an enlarged unit cell. Moreover, atoms on the B sites are occasionally short-range ordered within quenched chemical nanodomains with $Fm\bar{3}m$ symmetry [19]. The polar order parameter of PMN is directed along one of the eight rhombohedral $\langle 111 \rangle$ directions. Hence, an eight state Potts model might be applicable to this case. Fig. 2 shows the evolution of domains as simulated in a two-dimensional 4-state Potts model with respective planar RF s as a function of temperature [20]. At high temperatures, $k_B T/J = 10$, it is seen that the domains image the RF distribution, while on decreasing the temperature down to $k_B T/J = 0.2$ the domains become coarse grained and merely image the local fluctuations of the RF distribution. An appropriate means to evidence the nanoregions even when being dynamic, *i.e.* above any

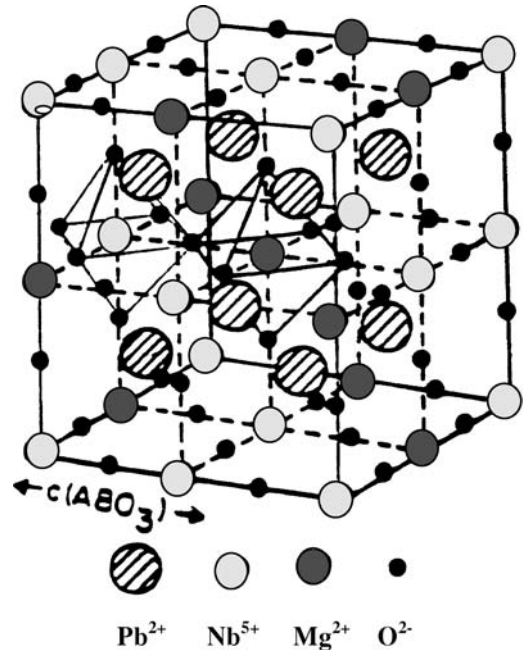


Figure 1 Random ionic distribution in PMN (Pb^{2+} = hatched circles, O^{2-} = small solid circles, Nb^{5+} = large solid circles, Mg^{2+} = open circles).

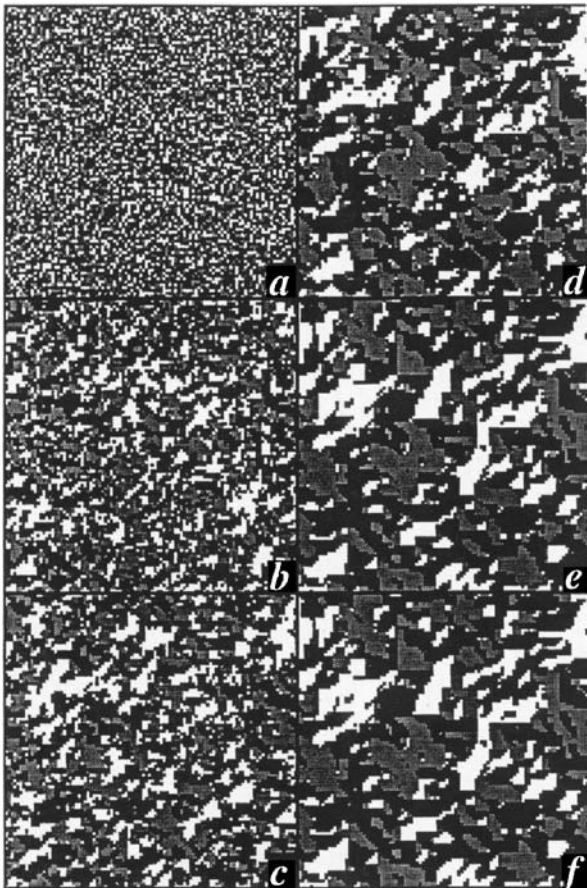


Figure 2 Domain distribution with polarizations $\pm P_x$ and $\pm P_y$ as indicated by different gray tones in a 4-state random field Potts model at temperatures $k_B T/J = 10$ (a), 1 (b), 0.8 (c), 0.6 (d), 0.3 (e) and 0.2 (f) (from [20]).

transition or freezing temperature, is the optical second-harmonic generation, SHG, as evidenced for both PMN [21] and SBN [22]. In both cases the SHG intensity starts to grow well above the transition temperatures.

Since the order parameter of PMN is close to be continuous, an equilibrium phase transition into a long-range ordered FE phase is excluded [9]. However, Blinc *et al.* [23] developed another route towards an ordered low- T phase. Based on the existence of polar nanoregions and their above described correlations, $q = \langle P_i P_j \rangle^{1/2}$ [16], they proposed a *spherical random bond RF (SRBRF)* theory. Here polar clusters of any size fulfilling the spherical constraint are considered as randomly interacting “*superspines*” which undergo a transition into a cluster glassy state. Theory has been solved for infinitely ranged interactions in mean-field approximation. Experimental tests by means of ^{93}Nb NMR reveal that the *RFs* are Gaussian distributed and that the Edwards-Anderson glass order parameter is finite below $T \approx 300$ K. Hence, no equilibrium static glassy freezing can be expected. Nevertheless, the preponderance of the random bonds with respect to the *RFs* clearly favors a glassy scenario which can be tested by measuring the (truncated) divergence of the nonlinear

susceptibility, χ_3 . More rigorously [24], the anisotropy parameter $a_3 = \chi_3/\chi_1^4$ has to maximize when approaching T_g on cooling, where χ_1 denotes the linear susceptibility. This has, indeed, been observed on both PMN and the related *relaxor* lead lanthanum zirconate-titanate (PLZT) [24].

A remark concerning the magnitude of the *RFs* seems in order. We are convinced that the primary function of the *local RFs* due to built-in charge disorder is to form energetically favored nanoregions [6]. These interact in a glass-like manner and form a spherical “*superspin*” glass [16, 23]. The glass transition, secondly, becomes smeared owing to *effective RFs*, h_i entering the *superspin* Hamiltonian, Equation 1. Since cluster spins containing N atomic spins experience only the fluctuations of the *local RFs*, the magnitudes of the *effective RFs* are reduced by factors $1/N^{1/2}$. This is why only weak smearing effects are observed. It should finally be remarked that the *SRBRF* theory has by far not yet generally been accepted. Still the origin of the nanoregions and their transition into a glassy state are disputed and not yet understood from a rigorous theoretical point of view. Clearly, the *RF* model simplifies the situation, since it neglects the possible relevance of bond disorder and the randomness of the quadrupolar degrees of freedom, which may give rise to structural glass behavior.

4. Uniaxial relaxors

In contrast to the cubic family related to PMN the polarization of the strontium-barium niobate family, $\text{Sr}_x\text{Ba}_{1-x}\text{Nb}_2\text{O}_6$, (SBN), is a single component vector directed along the tetragonal c direction, which drives the symmetry point group from paraelectric parent $4/mmm$ to polar $4mm$ at the phase transition into the low- T long-range-ordered polar phase as determined by X-ray diffraction [25]. Since SBN is tetragonal on the average, it belongs to the Ising model universality class rather than to the Heisenberg one as proposed for PMN-like system [6]. Assuming the presence of quenched random fields (*RFs*), available theory predicts the existence of a phase transition into long-range order within the *RF* Ising model (*RFIM*) universality class [9] preceded by giant critical slowing-down above T_c [11]. Only recently the SBN system has been found to fulfil the above necessary condition [13] and the ferroic *RFIM* seems to be materialized at last [26].

When explaining the unusual *relaxor* behavior, again the appearance of fluctuating polar precursor clusters at temperatures $T > T_c$ has to be considered as the primary signature of the polar *RFIM* [2, 3, 6]. Acting as precursors of the spontaneous polarization, which occurs below T_c , they have been evidenced in various zero-field cooling (ZFC) experiments comprising linear birefringence [27], linear susceptibility [28], dynamic light scattering

[29] and Brillouin scattering [30]. After freezing into a metastable domain state at $T < T_c$ the clusters were also directly observed with the help of high resolution piezoresponse force microscopy, PFM [31] (Fig. 3).

One of the major achievements provided by the discovery of the FE *RFIM* is the possibility to study the complete set of critical exponents on a ferroic system for the first time after their prediction [9, 10]. While most of the exponents compare well with predictions from theory and simulations [32], a remarkable deviation is found for the order parameter exponent, where $\beta = 0.14$ as determined by ^{93}Nb nuclear resonance [33] (Fig. 4) clearly deviates from the prediction $\beta \approx 0$ [32]. However, our value comes close to that observed recently on the standard *RFIM* system, the dilute uniaxial antiferromagnet $\text{Fe}_{1-x}\text{Zn}_x\text{F}_2$, $x = 0.15$, in an external magnetic field [34]. Further, the most disputed value, namely the specific heat exponent $\alpha \approx 0$ [35] clearly complies with the logarithmic divergence as

found on $\text{Fe}_{1-x}\text{Zn}_x\text{F}_2$ [10], which still lacks theoretical confirmation.

5. Domain dynamics in uniaxial relaxors

Domains in FE crystals are well-known to have a considerable influence on the value of their complex dielectric susceptibility, $\chi^* = \chi' - i\chi''$, and related quantities [36]. Owing to its mesoscopic character the domain wall susceptibility strongly reflects the structural properties of the crystal lattice. This is most spectacular in crystals with inherent disorder, where the domain walls are subject of stochastic pinning forces and χ^* is highly polydispersive due to a wide distribution of Debye-type response spectra [37, 38],

$$\chi^*(\omega) \propto \frac{\ln(1/\omega\tau_0)^{2/\Theta}}{(1+i\omega\tau)}, \quad (4)$$

where τ_0 and τ (with $\tau > \tau_0$), ω and $\Theta \approx 0.8$ (in $d=3$) are relaxation times, the angular frequency and a roughness exponent, respectively.

More generally, the dynamic behavior of domain walls in random media under the influence of a periodic external field gives rise to hysteresis cycles of different shape depending on various external parameters. According to recent theory [39] on disordered ferroic (ferromagnetic or FE) materials, the polarization, P , is expected to display a number of different features as a function of T , frequency, $f = \omega/2\pi$, and probing *ac* field amplitude, E_0 . They are described by a series of dynamical transitions between different “phases”, whose order parameter $Q = (\omega/2\pi) \oint P dt$ reflects the shape of the P vs. E loop being either zero or non-zero. When increasing the *ac* amplitude, E_0 , the polarization displays four regimes. First, at very low fields, $E_0 < E_\omega$, only “relaxation” with $Q = 0$, but no macroscopic motion of the walls occurs at finite frequencies, $f > 0$. Second, within the range $E_\omega < E_0 < E_{t1}$, a thermally activated drift motion (“creep”) is expected, while above the depinning threshold E_{t1} the “sliding” regime is encountered within $E_{t1} < E_0 < E_{t2}$. In both regimes $Q \neq 0$ is encountered. Finally, for $E_0 > E_{t2}$ a complete reversal of the polarization (“switching”) occurs in the whole sample in each half of the period, $\tau = 1/f$, hence, $Q = 0$. It should be noticed that all transition fields, E_ω , E_{t1} and E_{t2} , are expected to depend strongly on both T and f [39].

We have shown [40] that two different non-Debye responses corresponding to the field regions $E_0 < E_\omega$ (“relaxation”) and $E_\omega < E_0 < E_{t1}$ (“creep”) occur in the low- f dispersion of the uniaxial *relaxor* crystal $\text{Sr}_{0.61-x}\text{Ce}_x\text{Ba}_{0.39}\text{Nb}_2\text{O}_6$ (*SBN:Ce*, $x = 0.0066$) in the vicinity of its FE transition temperature, $T_c = 320$ K. It shows both characteristics in adjacent frequency regimes. While the well-known relaxational $\ln(1/f)$ characteristic

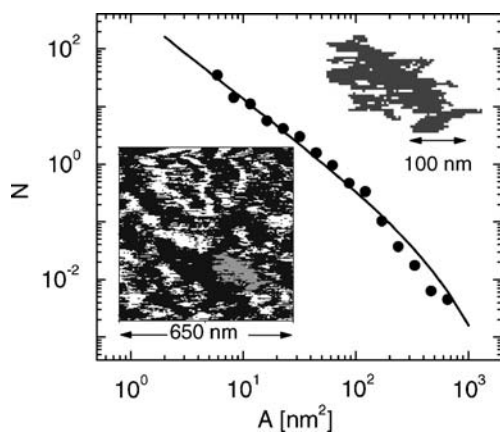


Figure 3 Spatial distribution of the ZFC surface polarization of *SBN61:Ce* ($x = 0.01$) (left-hand inset). Black and white areas refer to $\pm P_z$, respectively. One P_z domain (highlighted) is shown in the right-hand inset. The distribution function of domain areas A (solid circles) fits to the power law $N(A) = N_0 A^{-\delta} \exp(-A/A_\infty)$ with exponential cutoff and $\delta = 1.5$ (solid line) (from [31]).

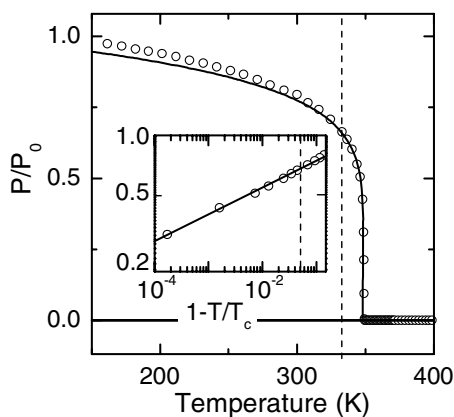


Figure 4 Order parameter of *SBN* as measured by NMR techniques displaying criticality with an exponent $\beta = 0.16$ (from [33]).

of relaxing domain wall segments in a weak random field [38] applies to “high” frequencies, $f > 100$ Hz, an alternative $1/f^\beta$ dependence is observed in the “low”- f regime, $f < 1$ Hz. In order to understand the latter behavior, we introduce polydispersivity via a broad distribution of wall mobilities, μ_w , which describe the viscous motion of the walls in the creep regime, where they overcome a large number of potential walls due to a high density of pinning defects. As a characteristic of irreversibility the walls stop when switching off the field. Within this concept the rapid individual Debye-type relaxation processes are averaged out on the long-time scale of a creep experiment. $(1/f)^\beta$ behavior at low frequencies has recently also been reported on the *relaxor*-type crystal $\text{PbFe}_{1/2}\text{Nb}_{1/2}\text{O}_3$ [41].

Dielectric response data were taken on a Czochralski-grown very pure crystal of *SBN*:Ce (size $0.5 \times 5 \times 5$ mm³) with probing electric-field amplitudes of 200 V/m applied along the polar c axis. A wide frequency range, $10^{-5} < f < 10^6$ Hz, was supplied by a Solartron 1260 impedance analyzer with a 1296 dielectric interface. Different temperatures were chosen both below and above T_c and stabilized to within ± 0.01 K. Fig. 5 shows representative data of χ' (curve 1) and χ'' vs. f (curve 2) taken at $T = 294$ K. They illustrate the main features of the dielectric dispersion of zero-field-cooled (ZFC) *SBN*:Ce: (i) the dielectric response strongly increases below $f_{\min} \approx 25$ Hz (marked by the dotted line); (ii) neither saturation of χ' nor a peak of χ'' are observed in the infra-low-frequency limit, where (iii) the magnitude of χ'' exceeds that of χ' by one order of magnitude; (iv) a Cole-Cole-type plot of χ'' vs. χ' is characterized by a positive curvature at frequencies $f < f_{\min}$ (Fig. 5; inset), which is opposite to the conventional Debye-type one; (v) at higher frequencies,

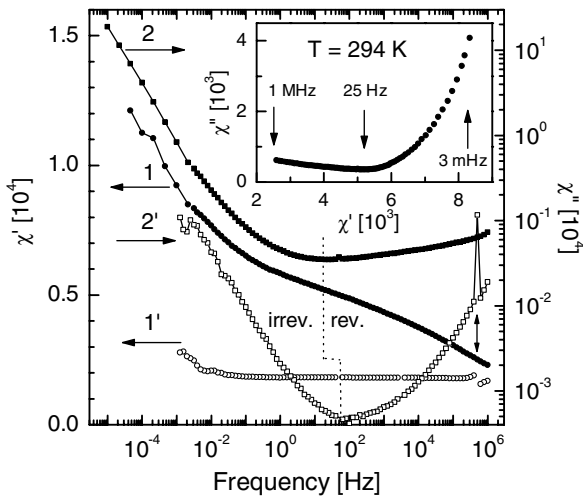


Figure 5 Dielectric spectra of χ' and χ'' vs. f of unpoled (curves 1 and 2) and poled (curves 1' and 2') *SBN*:Ce taken at $T = 294$ K. Solid lines are guides to the eye and the vertical dotted line separates different response regimes. A piezoelectric anomaly at $f = 0.5$ MHz is marked by a double arrow. The inset shows χ'' vs. χ' (from [40]).

$f > f_{\min}$, χ'' increases again in a power-law-like fashion (straight line in a log-log presentation), while χ' changes its curvature and gently bends down.

The dominating domain-wall nature of the response is evidenced by its drastic reduction when poling the sample with $E = 350$ kV/m from above T_c into a near-single domain state as shown by the curves 1' and 2' in Fig. 5. Despite its decrease by two orders of magnitude χ'' reveals, again, a symmetric increase on both sides of $f_{\min} \approx 65$ Hz (dotted line), which becomes power-law-like in the asymptotic low- and high- f regimes, respectively. This applies also to χ' (curve 1') after subtracting a background corresponding to the minimum at $f = 65$ Hz. Interestingly, a sharp piezoelectric resonance of both χ' and χ'' is observed at $f_{\min} \approx 0.5$ MHz after poling. This is typical of the near-single domain state, which activates a piezoelectric resonance.

The high- f response of both the ZFC and the FC states confirms many of the characteristics predicted by Equation 4. Inspection shows that χ' decreases linearly on a linear-log scale prior to the steeper decrease at $f > 10^4$ Hz, while χ'' obeys linearity on a log-log scale. Clearly, the ω prefactor strongly suppresses χ'' close to f_{\min} when compared with χ' . Upon increasing f the same factor determines the positive curvature of χ'' despite the competing $\ln(1/f)$ contribution (curve 2' in Fig. 5). Simultaneously, χ' is bent down in a dispersion step-like fashion.

While the high-frequency dispersion regime is attributed to polarization processes due to the reversible motion of domain-wall segments experiencing restoring forces, *viz.*, relaxation, the low-frequency response is due to the irreversible viscous motion of domain-walls. They experience memory-erasing friction by averaging over numerous pinning centers in a creep process. The latter type of motion becomes possible for at least two reasons: screening of depolarization fields by free charges in the bulk or at the surface and/or pinning of the domain-walls at quenched random fields, which is believed to be due to quenched charge disorder in the special case of *SBN*:Ce [13, 40].

Dielectric domain response under the action of an external electric field is readily modeled by considering the average polarization, $P(t) = (2P_s/D) x(t)$, of a regular stripe domain pattern of up and down polarized regions carrying spontaneous polarization, $\pm P_s$, and having an average width D . It arises from a sideways motion of walls perpendicular to the field direction by a distance x . Starting with $P(0) = 0$ at $x(0) = 0$, the favorable domains enhance their total width by an amount $2x$ until reaching (in principle) the limit $P = P_s$ for $x \rightarrow D/2$. By assuming viscous motion of the walls one obtains the rate equation

$$\dot{P}(t) = \left(\frac{2P_s}{D} \right) \mu_w E(t), \quad (5)$$

where the wall velocity $\dot{x}(t) = \mu_w E(t)$ involves the wall mobility μ_w and the driving field $E(t)$. Assuming constant mobility at sufficiently weak fields and disregarding the depinning threshold one finds

$$P(t) = \left[\frac{2\mu_w P_s}{i\omega\epsilon_0 D} + \chi_\infty \right] \epsilon_0 E_0 \exp(i\omega t). \quad (6)$$

under a harmonic field, $E(t) = E_0 \exp(i\omega t)$. In Equation 6 the second term refers to “instantaneous” response processes due to reversible domain-wall rearrangements occurring on shorter-time scales (see above).

The above relations are expected to hold in the limit of small displacements x , before the walls are stopped either by depolarizing fields (in conventional FEs) or by new domain conformations under the constraint of strong random fields (in disordered FEs). Weak periodic fields thus probe a linear ac susceptibility

$$\chi_w^*(\omega) = \chi_\infty \left(1 + \frac{1}{i\omega\tau_w} \right), \quad (7)$$

with $\chi_\infty/\tau_w = (2\mu_w P_s/\epsilon_0 D)$. The “relaxation” time τ_w denotes the time in which the interface contribution to the polarization equals that achieved instantaneously, $\Delta P = \epsilon_0 \chi_\infty E$.

Since the electric fields used in our experiments ($E_0 = 200$ V/m) are well below the coercive field, $E_c \approx 150$ kV/m, we have to account for the nonlinearity of v vs E in the creep regime, where thermal excitation enables viscous motion below the depinning threshold $E_{\text{crit}} \approx E_c$. Approximating this regime roughly by a power law $v \propto E^\delta$, $\delta > 2$, Equation 7 may be modified phenomenologically by introducing a Cole-Davidson-type exponent $\beta < 1$,

$$\chi_w^*(\omega) = \chi_\infty \left[1 + \frac{1}{(i\omega\tau_{\text{eff}})^\beta} \right], \quad (8)$$

similarly as used in the case of polydispersive Debye-type relaxation [42]. Here τ_{eff} denotes an effective relaxation time.

It has to be remarked that our approach neglects the hysteretic properties of the ac susceptibility, which are not contained in our adiabatic approach, Equation 6. This deficiency has been overcome in a recent approach based on a statistical model [43], where Equation 8 was deduced from the periodic motion of the domain walls in a randomly pinning medium on the basis of the quenched Edwards-Wilkinson equation. A similar result was recently obtained within a Rayleigh loop approach [44].

Decomposition of Equation 8 yields

$$\begin{aligned} \chi'(\omega) &= \chi_\infty [1 + \cos(\beta\pi/2)/(\omega\tau_{\text{eff}})^\beta] \quad \text{and} \\ \chi''(\omega) &= \chi_\infty \sin(\beta\pi/2)/(\omega\tau_{\text{eff}})^\beta \end{aligned} \quad (9)$$

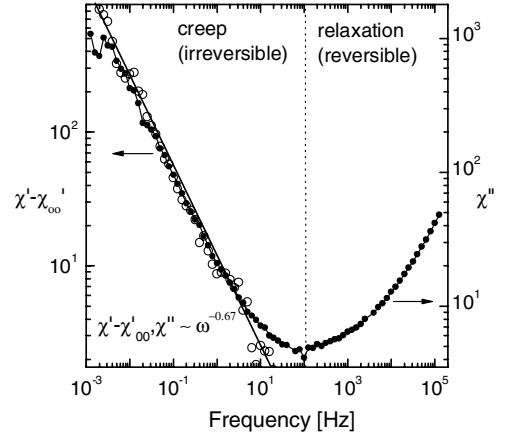


Figure 6 Dielectric spectra of $\chi' - \chi'_\infty$ (open circles), where $\chi'_\infty = 1820$, and χ'' (solid circles) vs. f of poled SBN:Ce taken at $T = 294$ K. The solid line is a best fit to Equation 6 and Equation 7 with $\beta = 0.67$ (from [45]).

such that

$$\chi''/(\chi' - \chi_\infty) = \tan(\beta\pi/2). \quad (10)$$

The power law-type spectral dependencies of χ' and χ'' are well supported by our experiments. While the unpoled sample exhibits an exponent $\beta \approx 0.2$ (not shown), *i.e.* large polydispersity, the poled sample yields $\beta \approx 0.67$ for both components of χ^* (Fig. 6) [45]. Obviously the polydispersity is largely suppressed at low domain wall densities. This seems to show that polydispersity is less affected by the nonlinearity in the creep regime, $v \propto E^\delta$ with $0 < \delta < 1$ in first approximation, than by the mutual wall interactions in the nanodomain regime [31]. Very satisfactorily, also the Cole-Cole plot, Equation 10, which is another independent test of the ansatz, Equation 8, reveals a very similar exponent, $\beta \approx 0.69$.

It should be noticed that the monodisperse relation, Equation 7, satisfies the Kramers-Kronig relationships, since $\chi'' \propto 1/\omega$ is a purely conductive contribution due to ohmic-like domain wall sliding and $\chi' = \chi'_\infty$ is constant. This is, however, no longer satisfied for $\beta < 1$, Equation 8. Hence, the spectral features displayed in Fig. 6 must necessarily change at very low frequencies. Here we conjecture - in accordance with the theory of dynamic phase transitions in random media [39] - that monodispersity, *i.e.* the sliding regime, should be attained asymptotically when approaching the static limit. This has recently been confirmed on the quantum-ferroelectric relaxor SrTi¹⁸O₃ in its domain state below $T_c = 25$ K [46].

6. Conclusion

The enigma of *relaxor* ferroelectrics seems to come close to be deciphered—50 years after the discovery of this remarkable material class [12]. Based on a vast amount of experimental and theoretical evidence it could be shown that the inherent charge disorder and its quenched random

electric field distribution must be at the very origin of *relaxor* behavior. The primary action of RFs is their correlating force onto the order parameter, which stabilizes polar nanoregions against thermal fluctuations [20]. This has been evidenced very clearly by high resolution PFM both on the uniaxial *relaxor* SBN [31] and, very recently, also on the cubic *relaxor*-like compound, PMN_{0.8}-PT_{0.2} [47].

However, since the ferroelectric phase transition in cubic *relaxors* like PMN is necessarily destroyed by arbitrarily weak RFs [9], random interactions between the different constituents of the solid solutions become relevant in these compounds. That is why cluster glassy scenarios are probably most appropriate for their description near to and below the freezing temperature [16, 23]. More research is needed to clarify the applicable model(s). The situation is much clearer in uniaxial *relaxors* like SBN, which is widely accepted to represent the first ferroic materialization of the 3d random-field Ising model [26]. Despite the clarity of this model and its consequences, future research is yet needed, e.g., for understanding details of the critical behavior when comparing experimental and theoretical results.

Acknowledgments

Work supported by the Deutsche Forschungsgemeinschaft via Forschungsschwerpunkt "Strukturgradienten in Kristallen".

References

1. M. E. LINES and A. M. GLASS, in "Principles and Applications of Ferroelectrics and Related Materials" (Clarendon, Oxford, 1977).
2. L. E. CROSS, *Ferroelectrics* **76** (1987) 241.
3. G. BURNS and F. H. DACOL, *Solid State Commun.* **48** (1983) 853; *Phase Trans.* **5** (1985) 261.
4. R. B. GRIFFITHS, *Phys. Rev. Lett.* **23** (1968) 69.
5. CH. BINEK and W. KLEEMANN, *Phys. Rev. B* **51** (1995) 12888.
6. V. WESTPHAL, W. KLEEMANN and M. D. GLINCHUK, *Phys. Rev. Lett.* **68** (1992) 847.
7. S. B. VAKHRUSHEV, B. E. KVYATKOVSKY, A. A. NABEREZHNOV, N. M. OKUNEVA and B. B. TOPERVERG, *Ferroelectrics* **90** (1989) 173; G. SCHMIDT, H. ARNDT, G. BORCHARDT, J. V. CIEMINSKI, T. PETZSCHE, K. BORMANN, A. STERNBERG, A. ZIRNITE and A. V. ISUPOV, *Phys. Stat. Solidi A* **63** (1981) 501.
8. K. BINDER and A. P. YOUNG, *Rev. Mod. Phys.* **58** (1986) 801.
9. I. IMRY and S. K. MA, *Phys. Rev. Lett.* **35** (1975) 1399.
10. D. P. BELANGER and A. P. YOUNG, *J. Magn. Magn. Mater.* **100** (1991) 272.
11. D. S. FISHER, *Phys. Rev. Lett.* **56** (1986) 416; A. T. OGIELSKI and D. A. HUSE, *Phys. Rev. Lett.* **56** (1986) 1298.
12. G. A. SMOLENSKI and V. A. ISUPOV, *Dokl. Acad. Nauk SSSR* **97** (1954) 653.
13. W. KLEEMANN, J. DEC, P. LEHNEN, T. H. WOIKE and R. PANKRATH, in: "Fundamental Physics of Ferroelectrics 2000", edited by R. E. Cohen, *AIP Conf. Proc.* **535** (2000) 26.
14. G. A. SAMARA, *Solid State Physics* **56** (2001), edited by H. Ehrenreich and F. Spaepen (Academic Press, New York, 2001) p. 240 and references therein; *J. Phys.: Cond. Matter* **15** (2003) R367.
15. D. SHERRINGTON and S. KIRKPATRICK, *Phys. Rev. Lett.* **35** (1975) 1972.
16. D. VIEHLAND, M. WUTTIG and L. E. CROSS, *Ferroelectrics* **120** (1991) 71; *Phys. Rev. B* **46** (1993) 8003.
17. A. BOKOV and Z. G. YE, *ibid.* **66** (2002) 064103.
18. P. BONNEAU *et al.*, *Solid State Chem.* **91** (1991) 350; L. E. CROSS, *Ferroelectrics* **151** (1994) 305; A. D. HILTON *et al.*, *J. Mater. Sci.* **25** (1990) 3461; T. EGAMI *et al.*, *Ferroelectrics* **199** (1997) 103; B. DKHIL *et al.*, *Phys. Rev. B* **65** (2002) 4104.
19. E. HUSSON, M. CHUBB and A. MORELL, *Mat. Res. Bull.* **23** (1988) 357.
20. H. QIAN and L. A. BURSILL, *Int. J. Mod. Phys. B* **10** (1996) 2027.
21. Y. UESU, H. TAZAWA and K. FUJISHIRO, *J. Kor. Phys. Soc.* **29** (1998) S703.
22. P. LEHNEN, J. DEC, W. KLEEMANN, TH. WOIKE and R. PANKRATH, *Ferroelectrics* **268** (2002) 113.
23. R. BLINC, J. DOLINSEK, A. GREGOROVIC, B. ZALAR, C. FILIPIC, Z. KUTNJAK, A. LEVSTIK and R. PIRC, *Phys. Rev. Lett.* **83** (1999) 424.
24. Z. KUTNJAK, C. FILIPIC, R. PIRC, A. LEVSTIK, R. FARHI and M. EL MARSSI, *Phys. Rev. B* **59** (1999) 294.
25. J. R. OLIVER, R. R. NEURGAONKAR and L. E. CROSS, *J. Appl. Phys.* **64** (1988) 37.
26. W. KLEEMANN, J. DEC, P. LEHNEN, R. BLINC, B. ZALAR and R. PANKRATH, *Europhys. Lett.* **57** (2002) 14.
27. P. LEHNEN, W. KLEEMANN, TH. WOIKE and R. PANKRATH, *Eur. Phys. J. B* **14** (2000) 633.
28. J. DEC, W. KLEEMANN, V. BOBNAR, Z. KUTNJAK, A. LEVSTIK, R. PIRC and R. PANKRATH, *Europhys. Lett.* **55** (2001) 781.
29. W. KLEEMANN, P. LICINIO, TH. WOIKE and R. PANKRATH, *Phys. Rev. Lett.* **86** (2001) 6014.
30. F. M. JIANG and S. KOJIMA, *Phys. Rev. B* **62** (2000) 8572.
31. P. LEHNEN, W. KLEEMANN, TH. WOIKE and R. PANKRATH, *ibid.* **64** (2001) 224109.
32. A. A. MIDDLETON and D. S. FISHER, *ibid.* **65** (2002) 134411.
33. R. BLINC, A. GREGOROVIC, B. ZALAR, R. PIRC, J. SELIGER, W. KLEEMANN, S. G. LUSHNIKOV and R. PANKRATH, *ibid.* **64** (2001) 134109.
34. F. YE, L. ZHOU, S. LAROCHELLE, L. LU, D. P. BELANGER, M. GREVEN and D. LEDERMAN, *Phys. Rev. Lett.* **89** (2002) 157202.
35. Z. KUTNJAK, W. KLEEMANN and R. PANKRATH, *Phys. Rev. B.* (submitted)
36. J. FOUSKEK and V. JANOVEC, *Phys. Stat. Sol. (a)* **13** (1966) 105.
37. L. B. IOFFE and V. M. VINOKUR, *J. Phys. C* **20** (1987) 6149.
38. T. NATTERMANN, Y. SHAPIR and I. VILFAN, *Phys. Rev. B* **42** (1990) 8577.
39. T. NATTERMANN, V. POKROVSKY and V. M. VINOKUR, *Phys. Rev. Lett.* **87** (2001) 197005.
40. W. KLEEMANN, J. DEC, S. MIGA, TH. WOIKE and R. PANKRATH, *Phys. Rev. B* **65** (2002) 220101R.
41. Y. PARK, *Solid State Commun.* **113** (2000) 379.
42. A. K. JONSCHER, in "Dielectric Relaxation in Solids" (Chelsea Dielectric Press, London, 1983).
43. A. A. FEDORENKO, V. MUELLER and S. STEPANOV, *Phys. Rev. B* **70** (2004) 224104.
44. D. DAMJANOVIC, S. S. N. BHARADWAJA and N. SETTER, *Adv. Mater.* (in print).
45. W. KLEEMANN, J. DEC and R. PANKRATH, *Ferroelectrics* **286** (2003) 21.
46. J. DEC, W. KLEEMANN and M. ITOH, *Ferroelectrics* **298** (2004) 163.
47. V. V. SHVARTSMAN and A. L. KHOLKIN, *Phys. Rev. B* **69** (2004) 014102.